

Satellite and radar analysis of the volcanic-cumulonimbi at Mount Pinatubo, Philippines, 1991

Andrew Tupper

Bureau of Meteorology, Darwin, Australia, and Monash University, Melbourne, Australia

J. Scott Oswalt

Long Beach, Mississippi, USA

Daniel Rosenfeld

Institute of Earth Sciences, Department of Atmospheric Sciences, Hebrew University of Jerusalem, Jerusalem, Israel

Received 8 October 2004; revised 31 January 2005; accepted 16 February 2005; published 11 May 2005.

[1] Several observers reported interesting convective phenomena in the months and years following the 15 June 1991 climactic eruption of Mount Pinatubo, Philippines. The observed phenomena included deep convection resulting from (1) lower level eruptions, (2) secondary phreatic explosions, and (3) enhanced surface heating. We have compared radar records and satellite imagery to obtain a more coherent understanding of these “volcanic-cumulonimbi” from 17 June to 30 September 1991 and to identify observational challenges for future events. Geostationary satellite imagery analysis for the period shows that the dominant localized effect on convection following the eruption was to bring the afternoon/evening peak in the diurnal convective cycle over the mountain forward by 2–3 hours. We examined four cases in detail and identified a number of possible interactions between the volcano and the meteorological environment. For three of these cases, the volcanic emissions apparently mixed with cumulonimbi developing around the volcano; on 21 June 1991, microphysical analyses clearly show a strong reduction in cloud top effective particle radius caused by the additional aerosols in the cloud, while on the two other occasions, there was a slight or barely detectable reduction. In the fourth case, for a cumulonimbus developing above a major secondary phreatic explosion, no unusually small cloud top effective radii were found, perhaps because the ash injected into the cloud was dominated by giant cloud condensation nuclei. These cases verify that volcanic emissions can be released through the depth of the troposphere and lower stratosphere from relatively small eruptions. Future major tropical eruptions and their aftermaths should be studied using intensive ground- and satellite-based observations to explore these phenomena further.

Citation: Tupper, A., J. S. Oswalt, and D. Rosenfeld (2005), Satellite and radar analysis of the volcanic-cumulonimbi at Mount Pinatubo, Philippines, 1991, *J. Geophys. Res.*, **110**, D09204, doi:10.1029/2004JD005499.

1. Introduction

1.1. Volcanic-Cumulonimbus and the 1991 Mount Pinatubo Eruption

[2] Study of the 1991 Mount Pinatubo eruption clouds has, justifiably, focused on the climactic 15 June event and its various impacts [Casadevall *et al.*, 1996; Guo *et al.*, 2004a, 2004b; Holasek *et al.*, 1996; Oswalt *et al.*, 1996; Robock, 2002; Tokuno, 1991]. Prelimactic eruption clouds have been relatively well documented [Hoblitt *et al.*, 1996; Lynch and Stephens, 1996; Potts, 1993], while discussion of the postclimactic activity has been more limited.

[3] For about a month following the climactic eruption, ash billowed continuously from vents in the Pinatubo

caldera [Wolfe and Hoblitt, 1996]. Secondary phreatic explosions caused by interactions between water and hot pyroclastic flow deposits for many years following the eruption [Holasek *et al.*, 1996; Oswalt *et al.*, 1996; Pinatubo Volcano Observatory Team, 1991; Torres *et al.*, 1996] may have also been responsible for much of the postclimactic “eruptive” activity within the caldera (S. Self and R. Torres, personal communication, 2005). Oswalt *et al.* [1996] also identified a group of phenomena that they termed “volcanic thunderstorms.”

[4] Oswalt *et al.* [1996] observed that during most of the postparoxysmal eruptions (or secondary phreatic explosions from the caldera), cumulus cloud complexes formed near the top of the buoyant ash plume, and then frequently developed further into cumulonimbi. These cumulonimbi often drifted away from their source region, producing significant amounts of rainfall, and ashfall. They also observed that significantly

greater than average amounts of afternoon convection occurred even in the absence of a buoyant volcanic plume, which they attributed to the influence of the hot pyroclastic flow deposits providing heating to the atmosphere and enhancing convective instability.

[5] The purpose of this paper is to further examine these fascinating phenomena. We first compare radar observations to satellite images and ancillary data during 17 June 1991 to 30 September 1991. We identify the area of enhanced convective activity using hourly cloud top temperatures during this period, and use the diurnal variation of cloud top temperatures to show how the volcano has enhanced normal orographic processes. We then consider the cloud development and the effect of volcanic aerosols on particle effective radius in four different situations, and we finally discuss the implications of these observations for volcanic cloud monitoring. Volcanic-cumulonimbi, or volcanic-Cb is used here as a general descriptor of the phenomena, including cumulonimbi formed over lower-level, postclimactic eruption clouds from vents in the Pinatubo caldera, over secondary explosions from the hot pyroclastic flow deposits around Mount Pinatubo, and over the hot pyroclastic flow deposits themselves.

1.2. Conceptual Models of Volcanic and Meteorological Convective Clouds

[6] The dynamics of volcanic eruption clouds are summarized by *Sparks et al.* [1997]. A volcanic eruption column can be conceptually divided into a small “gas thrust” region immediately above the vent where the column is dense and is driven upward by its inertia, a much deeper “convective region” where the column is less dense than the surrounding atmosphere and it rises because of its buoyancy, and an “umbrella region” where the column has come into equilibrium with the surrounding atmosphere and begins to spread out.

[7] Processes in the convective region are affected by the amount of latent heat release from entrained or preexisting moisture in the eruption column. Theoretical studies suggest that the state of the atmosphere can affect the height of rise of an eruption column by a few kilometers [*Graf et al.*, 1999; *Sparks et al.*, 1997; *Woods*, 1993, 1998]. The influence of entrained moisture is most marked for smaller eruptions; *Woods* [1993, p. 17,634] describes the small eruption columns as being “driven upward essentially as a result of the moist convection which they trigger.”

[8] Volcanic-Cb can be visualized as a form of triggered cumulonimbus [*Emanuel*, 1994], analogous to pyro-Cb [*Fromm and Servranckx*, 2003] but triggered by volcanic activity rather than wild fires, growing under normal convective processes with a minimal gas thrust region. In the tropics, the cold point tropopause is generally in the 16–17 km altitude range [*Seidel et al.*, 2001]. Allowing for occasional stratospheric penetration, volcanic-Cb could then extend as high as ~18–19 km above mean sea level.

[9] Pyro-Cb are capable of transporting large amounts of smoke aerosols into the lower stratosphere under favorable circumstances [*Fromm and Servranckx*, 2003; *Fromm et al.*, 2003], although it is unclear whether this mechanism is restricted to midlatitude supercell storms [*Wang*, 2003]. Modeled maritime tropical Cb have detrainment maxima at about 200 hPa (12–13 km) and 600 hPa (4–5 km)

[*Yasunaga et al.*, 2004]. Volcanic-Cb in the tropics are therefore potential sources of volcanic ash at these levels, and possibly higher. To date, however, apart from the observations of *Oswalt et al.* [1996], there have been virtually no reports of this kind of convection, possibly due to the practical difficulties of volcanic cloud observation in the moist tropics [*Tupper et al.*, 2004; *Tupper and Kinoshita*, 2003].

[10] Localized effects of volcanic-Cb can include “mud-fall,” flooding due to the rainfall generated, and the triggering of lahars (volcanic debris flows) [*Oswalt et al.*, 1996; *Pierson et al.*, 1996; *Rodolfo*, 1995]. Ash-bearing high-level cloud is also a serious hazard for aviation [*Casadevall*, 1994; *Johnson and Casadevall*, 1994]. There is now an international requirement for meteorological and aviation agencies to send real-time warnings of airborne ash as part of the International Airways Volcano Watch [*International Civil Aviation Organization*, 2000]. Although *Woods* [1993] noted that eruption columns driven by moist convection would have proportionally less ash at any altitude than those in dry atmospheres, the amount of ash required to damage aircraft is unknown. Recent aircraft encounters have included a case of an aircraft apparently being damaged when flying through a volcanic cloud so diffuse that only SO₂ was sensible, and that only by instruments [*Grindle and Burcham*, 2003]. There have also been other cases of clouds that have been sensible to the air crew but that have caused no damage [*Tupper et al.*, 2004].

[11] Observations of volcanic and other clouds should be considered in their meteorological context. Preferred areas for convective development are controlled by synoptic and mesoscale processes. Around mountains, there are at least seven identified orographic precipitation mechanisms, five of which can involve deep convection: (1) upslope triggering of convection, (2) upstream triggering of convection, (3) thermal triggering of convection, (4) leeside triggering of convection, and (5) leeside enhancement of convection [*Houze*, 1994]. Mesoscale processes significantly affect the transport of volcanic effluents [*Favalli et al.*, 2004; *Kinoshita et al.*, 2002]. To further develop our conceptual models of interactions between volcanic clouds and the environment, we must not only observe the convection, but also show how or if the volcanic activity has changed the convection patterns in the region of an active, ash-producing volcano. This is a considerable observational challenge.

2. Observational Methods

2.1. Meteorological Context

[12] The Philippines have a tropical maritime climate. The rainy season generally occurs from May to October in a southwest (summer) monsoon [*Dalida and Valeroso*, 1999; *Wu and Wang*, 2001], with a dry season from October to February in the northeast (winter) monsoon, and a transition season with a prevailing easterly flow during March to May [*Adug*, 2001]. Mount Pinatubo (elevation 1745 m before the eruption, 1485 m following the eruption) is in the southern part of the Zambales district in western Luzon (Figure 1), with its western slopes particularly exposed to southwesterly winds, creating a localized rainfall maximum during the summer monsoon [*Adug*, 2001; *Pierson et al.*, 1996]. The south-

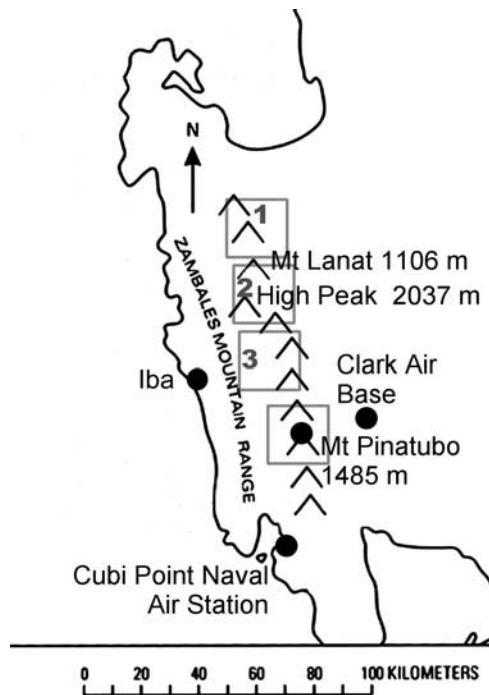


Figure 1. Location map (modified from *Oswalt et al.* [1996]). Numbered gray squares indicate regions of source data for comparison to Pinatubo area in Figure 4. Radars were placed at Clark Air Base and Cubi Point Naval Air Station.

west monsoon is often interrupted by either typhoon passage or “break” periods, causing torrential rain or more isolated diurnal activity respectively. The Zambales mountains have the late afternoon or early evening peak in convection characteristic of a southwest monsoon over topography [Dalida and Valeroso, 1999; Okumura et al., 2003].

[13] The June 1991 Pinatubo eruptions occurred in a year of weak El Niño and drought [Carello et al., 1994] but began just before the commencement of the southwest monsoon, and therefore much of the activity happened during heavy rain and low visibility for direct observations and remote sensing. The paroxysmal 15 June eruption itself coincided with the passage of a typhoon (locally named Diding, also known as Yunya after the Joint Typhoon Warning Center designation), which weakened to tropical storm strength during the eruption. The storm circulation had a strong effect upon the eruption’s tephra distribution and impact [Oswalt et al., 1996; Paladio-Melosantos et al., 1996]. From then until 30 September 1991, seven further tropical storms or typhoons came close to the northern Philippines [Joint Typhoon Warning Center, 1991].

[14] Original copies of 6-hourly, manual gradient level wind analyses for the period of study were obtained from the Darwin Regional Specialised Meteorological Centre in Australia. Atmospheric soundings and sounding diagnostics from Laoag (18.1°N, 120.3°E) and Legaspi (13.3°N, 123.7°E) meteorological stations were obtained from the University of Wyoming Department of Atmospheric Sciences (<http://weather.uwyo.edu/upperair/sounding.html>).

2.2. Radar Data

[15] The locations of the U.S. Navy and Air Force radars are shown in Figure 1. The radars were relatively old C band weather radars and are described in detail by *Oswalt et al.* [1996]. No printouts of screen displays could be taken from the radars, but detailed logs were kept during the eruptions, with over 490 nonzero plume height observations taken at Cubi Point during the 17 June to 30 September period. Although both radars had a maximum range of about 370 km, the real range was reduced by topography, and sometimes severely restricted by radar power fluctuations, or the presence of widespread echoes from volcanic or meteorological activity.

[16] A brief selection of 1991/1992 log entries is shown in Table 1. The uncertainties in methodology, the developing expertise of the observers, and importance of these observations are readily apparent. From the comparisons between Clark and Cubi Point radars in the logs, we estimate a random uncertainty of ± 3 km in the radar height estimates. Radar ceilings were 18.3 km (Cubi Point) and 24.4 km (Clark).

[17] The logs taken focused on the area above the vent; the height of material coming from the vent area was recorded as the height of eruption, although in practice it was difficult to distinguish between eruptions, secondary phreatic explosions and nonvolcanic cloud in the vent area without ancillary data such as direct observations or the often limited seismic information [Mori et al., 1996; Oswalt et al., 1996]. Convection occurring away from the vent was assumed to be nonvolcanic, except where it occurred near the new pyroclastic flow deposits and appeared to be outside the normal diurnal convective cycle, in which case it was sometimes identified as associated with secondary phreatic explosions. On rare occasions, it was possible to distinguish between ash and ordinary convection with experienced radar interpretation (e.g., Table 1, 25 September 1992).

2.3. Aircraft Observations

[18] The US Navy conducted helicopter and aircraft observation flights over the Pinatubo region during the months following the climactic eruption and into 1992. The observation flights were generally undertaken in the morning to avoid the afternoon instability and thunderstorm activity over the ranges, and for similar reasons were not possible during heavy monsoonal, volcanic, or typhoon activity. We have used video footage from a C-12 morning flight on 28 June 1991 in one of the case studies presented here. The C-12 (Huron) is a twin turboprop logistics aircraft.

2.4. Geostationary Satellite Data

2.4.1. Data

[19] Japan Meteorological Agency visible infrared spin-scan radiometer (VISSR) data [Meteorological Satellite Center, 1989] were obtained from the archives of the Australian Bureau of Meteorology, with a subsatellite resolution of 1.25 km (visible) and 5.0 km (infrared) and an hourly temporal resolution (an additional half-hourly image is taken every 6 hours in order to derive cloud drift winds). *Holasek et al.* [1996] describe the use of these data for documentation of the climactic eruption cloud. We exam-

Table 1. Selected Entries From Cubi Point Logs^a

Date	Entry
21 June 1991	0051UT weakened power is limiting range to ~10 miles. Lack of cells past 12 miles provides evidence that this is correct; therefore venting may be impossible to detect. 0202UT No venting noted; picking up 2 echoes around 20 nm out. Echoes weak. No other performance changes observed. 0255UT Unconfirmed report of eruption at 23Z–00Z, max tops reported to have been at 28,000 ft [8.5 km]. 0314UT No venting noted. 0758UT Minor venting to 20,000 ft [6.1 km] [Figures 7, 10, 11].
28 June 1991	0230UT Venting to 9,000 ft [3 km], 0245UT 15,000 ft [4.5 km], 0350UT 28,000 ft [8.5 km], 0410UT 30,000 ft [9.8 km], 0545UT 26,000 ft [8.5 km], 0555UT Ash cloud to 35,000 ft [11.5 km]. . . drifting west, 0625UT Venting to 23,000 ft [7.5 km]. Ash cloud dispersing but still visible to 22,000 ft [7.2 km] [Figures 5, 6, 10, 11].
8 July 1991	0025UT Venting up to 15,000 ft [4.5 km] is inducing Cbs over volcano through NW. Max tops 28,000 ft [8.5 km]. 0045UT Still inducing Cbs. Two cells one at 355° moving WNW max top 30,000 ft [9.1 km]. Second one at 010° stationary max top 32,000 ft [9.7 km].
14 July 1991	0625UT Cells starting to form in vicinity of Mount Pinatubo. Max tops 20,000 ft [6.1 km]. 0840UT Cells still in vicinity of Mount Pinatubo. It appears Mount Pinatubo is releasing a lot of steam and is inducing the cells around it.
15 July 1991	0415UT Venting to 12,000 ft [3.7 km]. Mount appears to be inducing the cells around it. Cells north and east max tops to 40,000 ft [12.2 km]. 0615UT Venting to 30,000 ft [9.1 km]. Ash cloud mixing with Cbs in vicinity moving WSW. Large cell 020° estimated 5 miles [8 km] from Cubi extending toward Mount Pinatubo max tops 60,000+ ft [18.3+ km]. 0650UT Hard to pick out venting height since ash and steam are mixing in with the rainshowers and thunderstorms [Figures 8, 10, 11].
16 July 1991	0500UT Venting masked by a 30,000 ft [9.1 km] Cb around Mount Pinatubo [until 0545Z]
18 July 1991	1355UT Possible venting/eruption to 40,000 ft [12.2 km]. No confirmation from Clark. They call it a rain shower – but have been getting ash all evening, getting echoes from up to 58,000 ft [17.7 km] east of volcano – 5 nm [9.3 km]. 1415UT Air Force still report thunderstorm. 1416UT Air Force finally decided it was an eruption. Cloud is heading east. 1430UT Eruption continues to 55,000 ft [16.7 km] – is broken up. Does not seem continuous. Echoes very strong [strong eruption continues, but at 1545UT radar masked by heavy rain until 1630Z]
12 Aug. 1991	0120UT Mount Pinatubo erupted. Informed by Clark weather, said to be up to 44,000 ft [13.4 km]. According to our radar it is up to 50,000 ft [15.2 km]. 0733UT Called Clark weather to confirm eruption of Mount Pinatubo. Clark weather says up to 38,000 ft [11.5 km]. Our radar confirms at 40,000 ft [12.2 km]. 1401UT Mount Pinatubo erupted. Informed by Clark weather, they say over 60,000 ft [18.3 km]. We are reading 51,000 ft [15.5 km]. . .
4 Sept. 1991	1991 0645 UT Venting to 60,000 ft [18.3 km] (Cb?). 0710UT Venting continues to 50,000 ft [15.2 km]. 0938UT Venting to 42,000 ft [12.8 km] being blown to the northeast by winds [Figures 9 and 10].
4 Aug. 1992	1149 UT Noted dense haze and large Cb NNE after observation, noted large area of echoes just east and west of Mount Pinatubo. Echoes were in excess of 60,000 ft [18.3 km]. Unable to determine whether echoes were precip, ash, etc. Called Pinatubo Volcano Observatory at Clark, no sightings or seismic activity there.
29 Aug. 1992	1545 UT Pinatubo area showing 40% coverage. . . Rapid rate of spreading and dispersion, assume SPE [secondary phreatic explosions]. Maximum top 45,000 ft [13.7 km], majority 25,000 ft [7.6 km].
25 Sept. 1992	1330 UT Possible SPE SW-NW of Pinatubo. . . Maximum top 40,000 ft [12.2 km]. Image very different (grainy, diffuse) from area of thunderstorms N through E of Pinatubo (Max 55,000 ft) [16.7 km].

^aFor readability, some abbreviations have been expanded, and comments are added in brackets.

ined all infrared and visible data from 17 June to 30 September 1991 using McIDAS 2002d (<http://www.ssec.wisc.edu/software/mcidas.html>).

[20] A parallax error in eruption cloud location was noted by Holasek *et al.* [1996]; this error arises because the navigation of an image is processed as if each point were at zero elevation on the surface of the Earth, and is particularly marked for stratospheric clouds such as from volcanic eruptions. In addition to this navigation issue, we observed a diurnally repeated, east-west navigation error of up to 60 km (navigation too far east in the midafternoon and too far west in the early morning), a smaller north-south navigation error, and random errors of 10–20 km. In some situations, especially where there was extensive cloud (such as during the climactic eruptions), it was impossible to correct the navigation of individual images. We therefore used relatively cloud-free images to empirically construct a time-dependent navigation correction function that was then applied to all images, leaving a residual uncertainty of ~20 km. In most of the individual cases described below, the uncertainty was very much lower (~5 km) because of the identification of topographic features in cloud-free parts of the images.

2.4.2. Satellite Identification of Individual Events of Interest

[21] GMS imagery can be used to detect 81.5% of “normal” eruption clouds above 10 km using pattern

recognition techniques [Sawada, 2003]. The detection rate for volcanic-Cb is almost certainly lower, because the albedo, dimensions, and general appearance of the clouds will be similar to normal Cb. To identify possible events, we examined each calibrated infrared or contrast-stretched visible image for the period 17 June to 30 September 1991 for evidence of isolated convection over the Pinatubo area. Only deep and optically thick convection was considered. The heights of the 77 identified discrete events were then determined using standard estimation methods [Holasek *et al.*, 1996; Lynch and Stephens, 1996]; primarily by wind drift and brightness temperature correlations. On the basis of uncertainties in the optical thickness of the clouds, ambiguities in the wind fields, and ambiguities in interpreting the temperature soundings, we estimate a height uncertainty of ± 2 km using these methods. This compares with the ± 1.3 km estimate of Holasek *et al.* [1996]. These results were then compared to the radar-derived heights described earlier and used in the selection of the case studies described in section 3.3.

2.4.3. Synthesis of IR Data for 17 June to 30 September 1991

[22] To examine the overall distribution and temporal variation of convection over the same period, we first eliminated all images with unusable data, prepared hourly composites of infrared cloud top temperatures over all days, and then created a synthesis of all hours. Because typhoon-

related clouds overwhelmed the volcanic signal in the cloud cover, *Joint Typhoon Warning Center* [1991] data were used to identify and eliminate all days where systems of tropical storm or typhoon strength affected the region (unfortunately, this means that some rain-induced secondary phreatic explosions, such as on 4 September 1991, were not used in the synthesis). After discarding bad or typhoon-related data, 1647 GMS-4 11 μm images were used in the final synthesis.

[23] This process was repeated for the same dates in a control year. Preeruption years are unsuitable for comparison because the topography of the area changed significantly in 1991, and years immediately after the eruption were also unsuitable because the secondary phreatic explosions continued for some years [Torres *et al.*, 1996]. The year 2002 was chosen because it was long enough after the eruption for all volcanic activity, including secondary phreatic explosions, to have ceased, and because the climatic conditions (a weak El Niño) make it a suitable analogue year [Carello *et al.*, 1994; Shaik and Jackson, 2003]. After eliminating tropical storm or typhoon affected days [Joint Typhoon Warning Center, 2002] and bad data, 2180 GMS-5 11 μm images were used in the 2002 synthesis.

2.5. NOAA AVHRR Data

2.5.1. Data

[24] NOAA 10 and 11 advanced very high resolution radiometer (AVHRR) data [National Oceanic and Atmospheric Administration, 1998] were retrieved from the NOAA Satellite Active Archive (<http://www.saa.noaa.gov/>). AVHRR data have channels with central wavelengths 0.64, 0.83, 3.7, 11, and 12 μm (NOAA 10 data lack 12 μm). Data from this region and period are generally only available in 4 km global area coverage format because of a lack of reliable local receivers, but during the Pinatubo crisis, NOAA activated the satellites' onboard recorders to record local area coverage (LAC) format images with 1.1 km nominal resolution.

[25] We performed multispectral analysis on the majority of the two images per day from each operational satellite, focusing on daytime events. Twenty-one of these images coincided with the events already identified from GMS-4 images, during 17 June to 30 September 1991.

2.5.2. Multispectral Techniques

[26] Single visible or infrared channels are often effective for volcanic cloud detection [Sawada, 1987, 2003], but multispectral techniques are generally used when possible. Two principal techniques were used. For dispersing, non-opaque clouds, we used "reverse absorption" [Prata, 1989a, 1989b], using 11 and 12 μm channels, which in this case were only available on NOAA 11. Limitations of this technique include the absorptive effect of high levels of water vapor [Potts, 1993], and the masking effects of high amounts of water/ice in the eruption clouds [Rose *et al.*, 1995]. Reverse absorption was successfully used to identify ash during the Pinatubo eruptions [Casadevall *et al.*, 1996; Guo *et al.*, 2004a; Potts, 1993], and despite its limitations is an effective operational tool for monitoring ash clouds in the region [Tupper *et al.*, 2004]. Guo *et al.* [2004a] tracked fine ash (1–12 μm) particles for 104 hours after the main Pinatubo eruption using AVHRR data and the reverse absorption technique.

[27] The 3.7 μm channel has also successfully been used for volcanic cloud detection, either as an alternative to 12 μm when using reverse absorption for ash rich clouds [Ellrod *et al.*, 2003], or as a daytime reflective band for ash-poor clouds that nevertheless have smaller particle sizes and therefore different reflective properties [Kinoshita *et al.*, 2002]. Recent work has shown that ash particles entrained into dense, ice-rich meteorological cloud can cause a smaller effective particle radius in the cloud top (D. Rosenfeld and A. Tupper, Volcanic eruptions revealed through ash affecting satellite-inferred cloud properties, manuscript in preparation, 2005, hereinafter referred to as Rosenfeld and Tupper, manuscript in preparation, 2005), implying a possible method of detecting volcanic ash in these clouds. The magnitude of the effect is dependent upon the flux of particles into the cloud. The effective radius retrievals are limited to a maximum size of 35 μm , because the 3.7 μm reflectance decreases to near the instrument noise level for clouds of larger particles [Rosenfeld and Lensky, 1998].

3. Results

3.1. Comparison of Radar and GMS-4 Heights

[28] Figure 2 summarizes the radar-derived cloud heights, GMS-4-derived maximum heights of events identified during the analysis process, and the periods during which typhoons or tropical storms affected the region. The satellite and radar observations are quite independent, consistent with the different foci and temporal and spatial resolutions of the data. In many cases the events will have been observed at slightly different times, and what may have been perceived as individual cells on the radar may look like one storm on satellite images. Also, the radar observations include many lower-level (below 10 km) events that were not observed clearly with GMS-4, partly due to the tendency of cirrus from high-level convection to spread near the tropopause, last for some hours, and obscure lower-level events.

[29] In general, the GMS-4 images of these events demonstrated few unusual characteristics apart from the frequency and persistence of deep convection over the site, which was often obviously associated with low-level (1–5 km) plume activity. In contrast to the preclimactic and climactic eruptions, no high-altitude low-albedo features (indicating highly ash dominant aggregates) were observed on visible images.

[30] Overall, the height estimates show a clustering of the deep convection around the tropopause or 1–2 km below, with a few events penetrating into the lower stratosphere. Where the same event is observed by satellite and radar, the maximum cloud heights from each instrument are usually within a few km of each other, consistent with our estimated uncertainties. The greater heights indicated by radar observation of the highest clouds may be caused by radar inaccuracy at these altitudes, but may also reflect the greater temporal resolution of the radar, which gives a better chance of seeing these extreme events at their apex, and the often small temperature gradients around the tropopause, which make it difficult to resolve infrared features penetrating just into the stratosphere. This overall distribution is characteristic of normal convection in the moist tropics. It was also quite common to see thunderstorms in the wider area

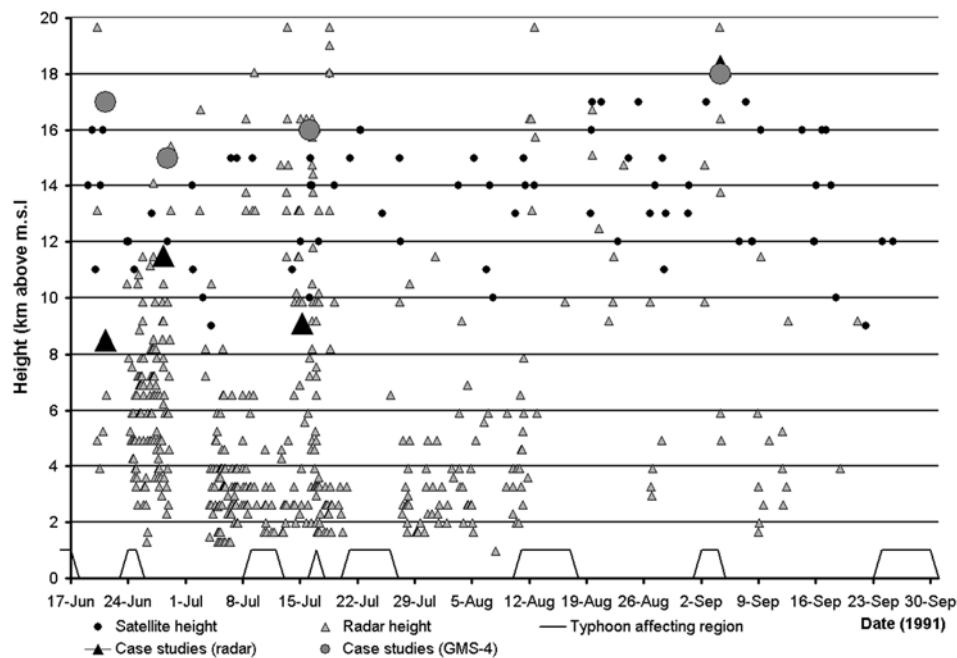


Figure 2. Summary of convective events over the Pinatubo region during 17 June to 30 September 1991, comparing GMS-4-derived heights (small circles) with radar observations (small triangles) over the vent. Periods where tropical storms or typhoons were affecting the region are marked (solid line at bottom). The four case studies are shown as large circles and triangles for their maximum height on satellite and radar data, respectively.

penetrating into the stratosphere. For example, on 9 September 1991 at 06:40 UT, a storm to the north of the region of interest was 8.4K warmer in the center than at the edge of the cold overcast, corresponding to an altitude of approximately 18 km, 2 km above the tropopause, assuming the cloud temperature was in equilibrium with its environment.

[31] Some events could confidently be identified as convection over secondary phreatic explosions, venting or eruptions, when convection was initiated in very unusual situations (such as through the cirrus shield around a typhoon) over Pinatubo. Holasek *et al.* [1996] have shown such an image for 4 September 1991. Similar events occurred on 18 July (Table 1), 22 July (no radar confirmation due to power problems), and 12 August (Table 1). Secondary pyroclastic flows and associated phreatic explosions on 12 August and 4 September 1991 are described by Torres *et al.* [1996]; these events were thought by operators at the time to be from the crater but probably occurred 5–10 km away over the pyroclastic flow deposits from the circumstantial evidence.

[32] Four case studies have been highlighted with large symbols in Figure 2. The first three of these had satellite observed heights far in excess of the radar-observed height, suggesting that the peak convection height was not directly attributable to activity at the volcano; the fourth is for the 4 September 1991 event. These cases are discussed in section 3.3.

3.2. Satellite Analysis

3.2.1. Spatial and Diurnal Variation of Mean Cloud Top Temperatures

[33] Figure 3a shows the extent of the identifiable enhanced activity. The coldest mean cloud tops during 17 June

to 30 September 1991 over the Philippines region were over the Pinatubo region. The westward extension of the cold area is consistent with the mean direction of travel of deep convection forming over the Philippines, resulting from deep easterly “steering” winds. Another cold minimum near 13N 120E reflects a highly favorable zone for nocturnal maritime convection, possibly caused by land-breeze convergence, combined with afternoon activity advected from Mindoro. This Mindoro minimum is slightly more pronounced in the 2002 data (Figure 3b), but there is no enhanced activity at all over Pinatubo in 2002.

[34] The diurnal variations of radar-derived cloud heights above Pinatubo are shown in Figure 4a. The radar data are somewhat noisy, but the mean hourly heights and the number of events reaching over 5 km in height suggest a diurnal cycle of cloud height over the vent, with larger events tending to be in the late afternoon and evening.

[35] A diurnal variation is much more apparent in the satellite analysis (Figure 4b). Here the hourly variation cloud top brightness temperature in a 20×20 km box centered on Pinatubo is compared to the average of three other locations in the Zambales range, which is topographically and climatologically similar, to the thunderstorm climatology of Dalida and Valeroso [1999], and to the Pinatubo area in 2002. The Zambales range in general has the late afternoon or early evening peak in convection characteristic of a southwest monsoon over topography in the region [Dalida and Valeroso, 1999; Okumura *et al.*, 2003]. In Figure 4b, the diurnal variations in mean cloud top temperature for areas 1–3 (see Figure 1), and for the Pinatubo area in 2002, closely match the climatological thunderstorm occurrence at the nearby Iba meteorological station. The cloud temperatures over Pinatubo in 1991 were

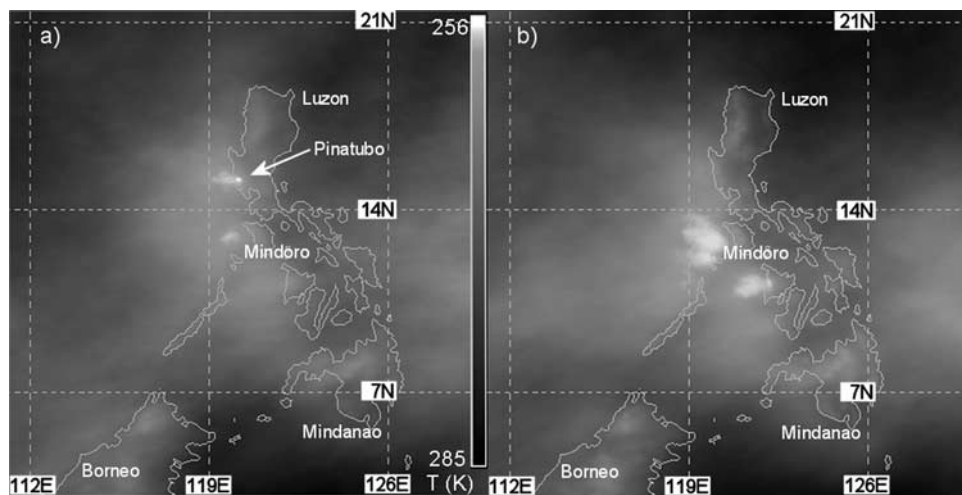


Figure 3. (a) Mean brightness temperatures using GMS-4 data for 17 June to 30 September 1991, and (b) using GMS-5 data for 17 June to 30 September 2002, for all hours, but excluding days with widespread tropical storm or typhoon cloud, and also excluding bad and redundant data. The effect of the postclimatic activity at Pinatubo in 1991 can be clearly seen.

generally colder for all hours, as expected from Figure 3a. More interesting, however, is that where we might expect a slight “flattening” of the diurnal trend because of the more randomly distributed eruptions, or a lengthening of the afternoon peak or a secondary morning peak due to rain-induced secondary phreatic explosions, there is no such result. Instead, the effect of the postclimatic eruption environment on convection appears to have been to bring the early evening convective maximum forward by 2–3 hours.

[36] We interpret these results as reflecting a tropical environment that is still essentially controlled by diurnal, orographic heating mechanisms, but where there are factors contributing to a faster than usual decay of early convective inhibition during the day. In this case, the factors could include (1) the elevated temperature of the pyroclastic flow surfaces around Pinatubo, venting from the caldera and secondary explosions from the deposits providing additional heat and moisture, inducing continuous shallow convection and mixing out nocturnal inversions, (2) instability created by absorption of radiation by dark particles at the top of ash-rich plumes, analogous to the Kuwait oil fires [Rudich *et al.*, 2003], and (3) fast heating of the new, bare volcanic material exposed to the sun. Of these, factors 1 and 2 depend to some extent on the amount of volcanic activity. The radar results suggest that diurnal mechanisms may have affected even observations designed to observe eruptive activity.

3.2.2. Reverse Absorption Analyses

[37] In the first two to three weeks following the climatic eruptions, many images showed a continuous plume at low levels (1–5 km) from the Pinatubo area. During July these images became less frequent as the venting slowly eased and the atmospheric conditions leading to good plume visibility (a relatively dry atmosphere with moderate to fresh winds underneath an inversion at 3–5 km) became rare. However, in contrast to the period of main eruptions [Guo *et al.*, 2004a], no ash at high levels was explicitly sensed using reverse absorption. We infer from these results that substantial levels of fine ash did not generally exist at

high levels unless as part of ice/ash aggregates, or as free ash but with a reverse absorption signal overwhelmed by the ice signal [Guo *et al.*, 2004a; Rose *et al.*, 1995].

3.3. Case Studies

[38] Four of the 21 considered case studies during the target period are presented here. We describe the meteorological environment and ancillary observations for each case (Figures 5–9, Table 2), summarize the main potential triggering mechanisms for deep convection in the potentially unstable atmosphere in each situation (Figure 10), and then show results of particle effective radius analysis (Figures 11 and 12).

3.3.1. The 28 June 1991 Case

[39] Figure 5 shows convection observed by the US Navy over the Pinatubo region early (00 UT) on 28 June. This flight occurred during a break in the monsoon, with consistent easterly winds of 10 m/s through most of the troposphere. Convective Inhibition and Convective Available Potential Energy (CAPE) [Emanuel, 1994] were both moderate, and deep convection was quite isolated until the late afternoon (Table 2). The morning convection over Pinatubo was the only substantial convection in the area at the time. Radar observations (Table 1) showed the convection height building during the day, with an “ash cloud” observed to 11.5 km at 0555 UT. At the time of Figure 5, radar and satellite observations, and the video evidence, suggests that the cumulus height was 3–5 km above mean sea level (amsl), or at any rate below the freezing level (5 km).

[40] The low-level ash detrained from this convection can be seen in Figure 6, which shows visible and reverse-absorption images from 0618 UT. Assuming the measured winds are representative, the ash near “1” is about 6 hours old and derives from about the time of Figure 5 (0000 UT), with variations in plume width and opacity reflecting changes in ash emission. The ash emissions appear white, whereas the water/ice clouds appear gray in Figure 6b. At the site of the eruption, deep convection “2” has developed, to about 15 km amsl. Cold cumulonimbus clouds often have a

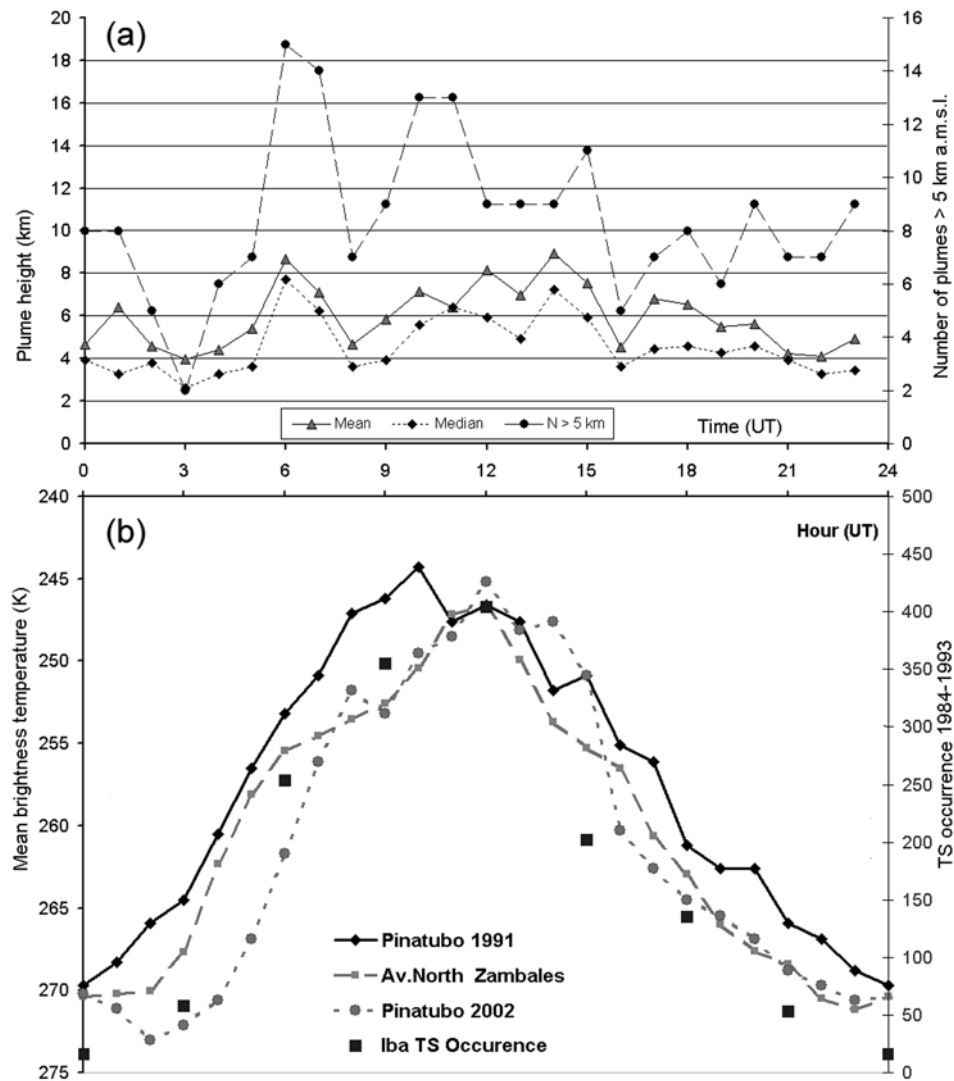


Figure 4. (a) Mean and median diurnal heights for each hour from Cubi Point radar records and (right y axis) number of occasions from 17 June to 30 September 1991 when plume above vent exceeded 5 km above mean sea level in height. (b) Diurnal variation of mean brightness temperature, using same data as for Figure 3, for Mount Pinatubo area in 1991, the average of three adjoining areas over the rest of the Zambales (see Figure 1) in 1991, and for the Pinatubo area in 2002. Solid squares (right y axis) give the mean thunderstorm occurrence at Iba (Figure 1) during the southwest monsoon season, based on 1984–1993 data from *Dalida and Valeroso* [1999] (right y axis). The Zambales area in 1991 and the Pinatubo area in 2002 are quite consistent with thunderstorm climatology, but the Pinatubo area in 1991 shows a marked and earlier diurnal peak in activity. Philippine local time is UT + 8.

zero brightness temperature difference on reverse-absorption images [Prata, 1989a], but can be distinguished from semiopaque ash cloud using “scatter diagrams” (not shown) [Prata *et al.*, 2001]. GMS image animations suggest that these storms are related to an earlier tropical squall line, which developed over central Luzon earlier and moved westward with the middle-level winds. The cumulonimbi over Pinatubo may therefore have mixed origins, with lower-level eruption cloud being incorporated into the tropical squall line.

3.3.2. The 21 June 1991 Case

[41] Following the climactic eruption of Pinatubo and the passage of the typhoon, a southwest monsoon surge affected the region with fresh to strong winds, and a consequent

increase in convective activity over western Luzon. On 21 June, northern Luzon was entirely covered in middle level cloud, with deep cumulonimbus over the Zambales range and offshore to the west, and strong southeast winds near the surface (Figure 7). Convective inhibition was very small (Table 2), and the moist onshore flow piling up against the Zambales range created a favorable environment for sustained convection. Under these conditions, visual surface observations would have been very difficult at Pinatubo, and the radar power fluctuations at Cubi Pt in the morning (Table 1) and limited seismic data [Mori *et al.*, 1996] restricted remote observations. However, the blow off of cirrus toward the west in brisk upper level easterly winds (Figure 10) allowed some GMS-4 observation of the regions

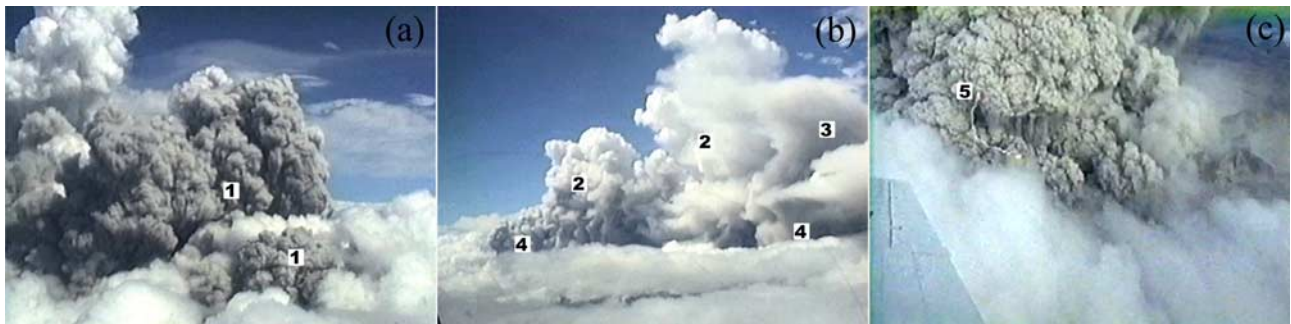


Figure 5. Video stills of convection over Pinatubo from U.S. Navy C-12 reconnaissance flight, ~0000 UT 28 June 1991. Features highlighted are (1) discrete ash/water cumulus breaking through water-rich cumulus near the vent, (2) gradual transition of ash-rich cumuli to more ordinary looking cumuli as heavier ash falls out with height, (3) “glaciated” appearance of older cloud as the updraft collapses and the cloud detrains ash, (4) “cave-in” at sides of cloud as ash-fall-induced downdrafts cause stabilization, and (5) volcanic lightning in ash-rich and apparently unglaciated cumulus.

of deep convection initiation over the Zambales range. Convection to high altitudes was semicontinuous over the Pinatubo region from 1430 UT on 20 June to 1130 UT on 21 June, with a maximum height of 19 km at 0640 UT, 2 km above the tropopause. Animation of the morning’s GMS-4 imagery suggests that the Pinatubo region was more active than other locations, presumably due to some volcanic enhancement of the orographic convection.

3.3.3. The 15 July 1991 Case

[42] The 15 July 1991 case occurred in a similar monsoon break period to 28 June. A weak high-pressure system just west of Luzon extended a ridge across the Philippines (Figure 8), and light northeasterly winds prevailed through the depth of the troposphere. The relatively low CAPE (Table 2) and suppressing effect of the ridge kept deep convection very isolated until the afternoon. At this stage of the postclimatic period, the continuous emissions of fine ash from Pinatubo had noticeably decreased and no plume was visible on satellite images.

[43] By 06 UT, deep convection had developed over many parts of northwest Luzon. Earlier GMS-4 0430 UT images show that the initial development at Mount Pinatubo was more widespread and was deeper than at other locations, supporting the Cubi Point observer’s comment that the mountain “appears to be inducing the cells around it” (Table 1). By 0615 UT, Cubi Point was reporting that the ash clouds (to 9 km) from the Pinatubo vent were mixing with the cumulonimbi (to heights over 18 km, Table 1).

3.3.4. The 4 September 1991 Case

[44] *Holasek et al.* [1996] showed a NOAA AVHRR image of a deep convective cloud (height ~ 18 km) apparently generated over a secondary pyroclastic flow and related secondary phreatic explosion in the Marella River, about 7 km to the southwest of the crater on 4 September [Torres *et al.*, 1996]. Figure 9 shows the synoptic situation on this day, which bears many similarities to that of 21 June, but with a much deeper southwesterly monsoon flow (Figure 10). Tropical storm Joel was at minimal strength, with a large area of fresh to strong winds to the south, and deep orographic convection along the coast. The torrential rain from this convection, together with the secondary phreatic explosions induced by the rainfall, was responsible for the ash remobilization at Pinatubo. A large

cumulonimbus or complex of cumulonimbi formed over Pinatubo during the afternoon, and then advected to the northeast in 10 m/s steering winds. Although the secondary pyroclastic flow was not directly observed at the time, the timing was reckoned from the timing of the Cb, and associ-

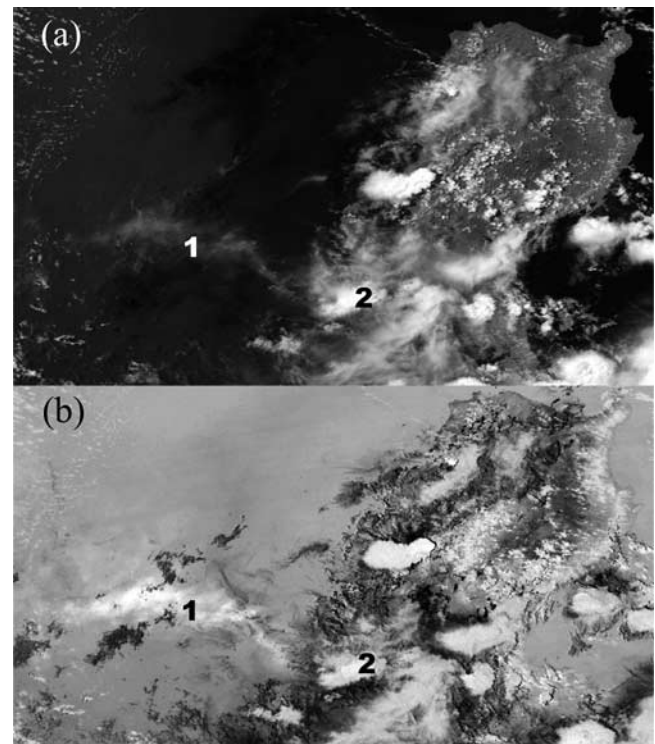


Figure 6. NOAA 11 AVHRR, 28 June 1991, 0618 UT, (a) 0.85 μm and (b) 12–10.8 μm “reverse absorption” image, showing (1) lower-level ash plume extending ~300 km to the west (bright on both images), and (2) cold ash/ice clouds over Pinatubo. In a reverse absorption image from AVHRR data, volcanic ash, mineral dust, and very cold, dense Cb tops will appear bright, and thin cirrus and lower-level clouds will appear dark. The IR-derived height of cloud 2 was ~15 km, and the maximum ash cloud height observed by radar was 11.5 km.

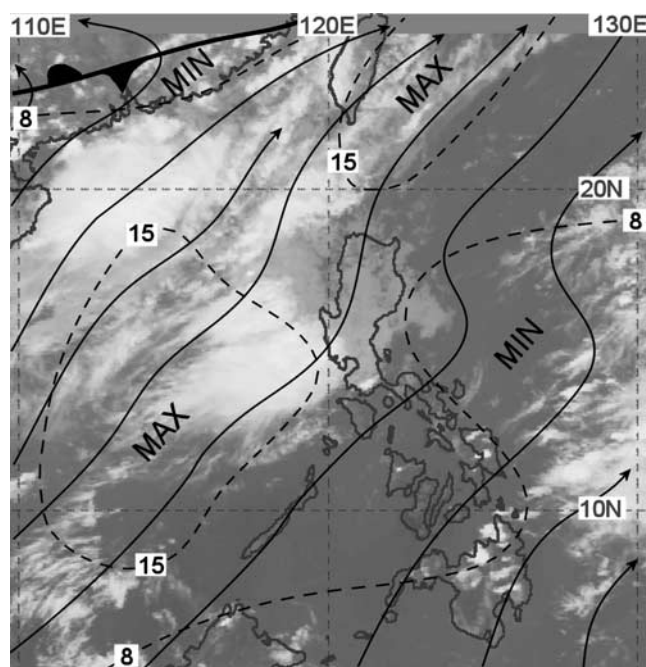


Figure 7. GMS-4, 21 June 1991, 0541 UT, infrared image, with gradient level streamlines and isotachs (m/s) overlaid from Darwin RSMC 0600 UT analysis.

ated ash fall to the east and northeast of Pinatubo [Torres *et al.*, 1996]. Few secondary explosion clouds came close to or exceeded the volume, and perhaps mass remobilization rate, of this event (R. Torres, personal communication, 2004).

3.3.5. Convection Triggering Mechanisms

[45] From the known activity at the volcano, and the synoptic and radar data and satellite analysis, Figure 10

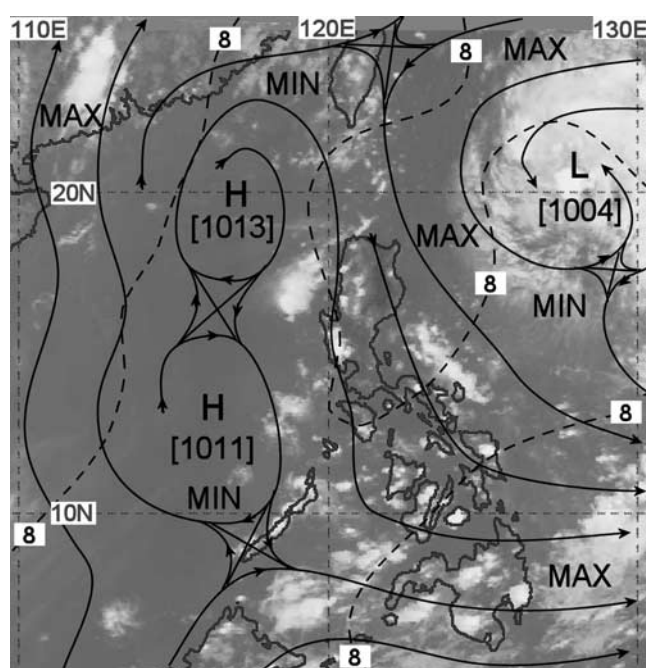


Figure 8. GMS-4, 15 July 1991, 0541 UT, infrared image, with gradient level streamlines and isotachs (m/s) overlaid from Darwin RSMC 0600 UT analysis.

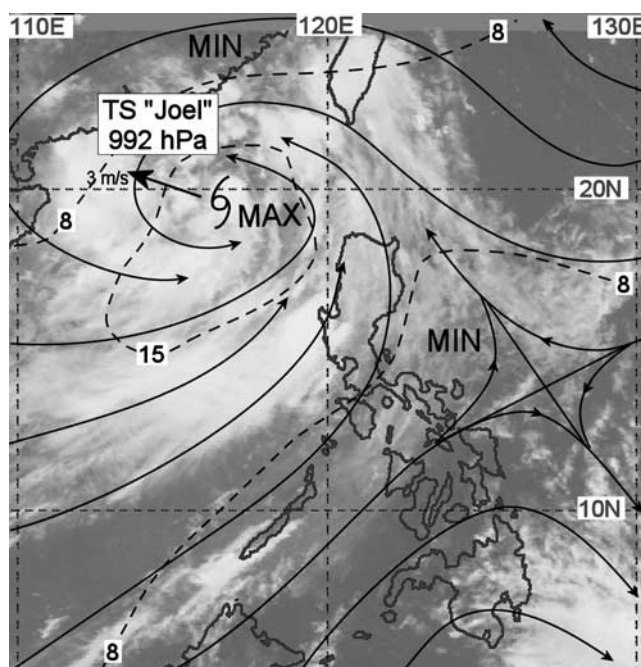


Figure 9. GMS-4, 4 September 1991, 0511 UT, infrared image, with gradient level streamlines and isotachs (m/s) overlaid from Darwin RSMC 0600 UT analysis.

summarizes the presumed convection triggering mechanisms in the Pinatubo area for these four cases. Volcanic processes over the central vent are presumed to have been factors for the first three cases; by September, activity at the vent had virtually ceased and secondary phreatic explosions had taken over as the dominant volcanic mechanism. Upslope or upstream triggering of convection may have been a factor for all cases except 15 July, when winds were very slight. Cold convective outflow may have helped trigger convection above the volcano on 28 June as the preexisting squall line moved westward. The ash-laden cold outflow from the convection over the volcano on 15 June may have also induced the deep convection to the west. Mesoscale heating of the elevated topography was probably a factor on all occasions, but more so on 28 June and 15 July, which were relatively cloud-free days. The radar

Table 2. Selected Sounding Indices From Laoag Station in Northern Luzon (World Meteorological Organization 98223), for the Days of the Four Case Studies^a

	28 June 1991	21 June 1991	15 July 1991	4 Sept. 1991
CAPE, J/kg	1430	1168	302	83
Convective inhibition, J/kg	-150	-5	-177	-61
Level of free convection, hPa/approximate km	709/3.0	883/1.4	654/4.5	486/6.0
Level of neutral buoyancy, hPa/approximate km	160/14	147/14	290/10	372/8.2
Cold point tropopause, hPa/approximate km	98/17	102/16.5	101/16.6	104/16.4
Precipitable water, mm	50	68	49	53

^aThe stability indices have been calculated using virtual temperature. Data are courtesy University of Wyoming, Department of Atmospheric Sciences. CAPE, convective available potential energy.

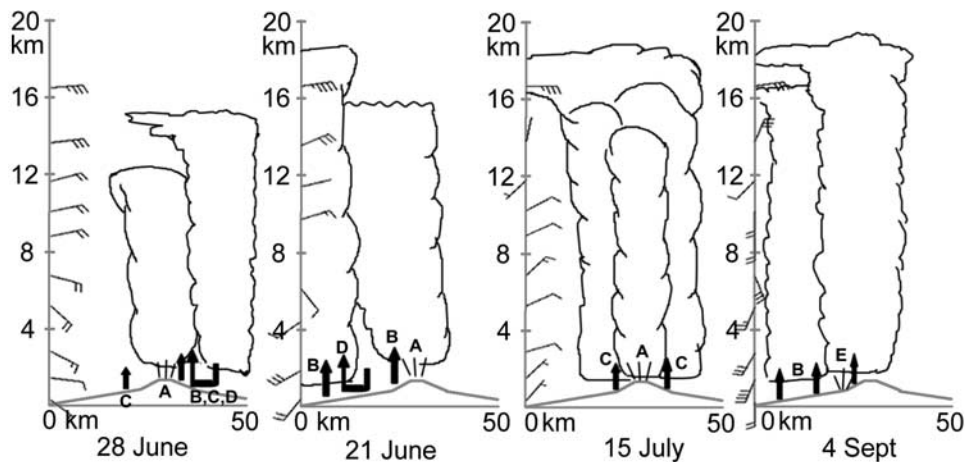


Figure 10. Schematic (with simplified topography) of presumed main convection triggering mechanisms for the four cases studied here: A, heating, eruptions, or secondary phreatic explosions from the vent area; B, upslope or upstream triggering of convection [Houze, 1994]; C, uplift from diurnal mesoscale heating; D, outflow from existing convection; E, secondary explosions on the flank of the volcano. The sketches are overlaid on wind profiles from Laoag meteorological station, using normal meteorological conventions: each full barb on the staff is 10 knots (5.1 m/s), and the staff points toward direction of movement of the wind. Wind data are courtesy University of Wyoming, <http://weather.uwyo.edu/upperair/sounding.html>.

observations from 21, 28 June and 15 July suggest that the cloud actually observed over the vent was lower than the eventual maximum height of the convection. The next question to investigate is whether the ash lifted in these clouds can be detected in the cloud tops.

3.3.6. Microphysical Analysis

[46] Figure 11 shows the microphysical rendering of AVHRR images for these four cases, and Figure 12 shows temperature/effective radius (r_E) analyses for four selected areas of Figure 11. In general, the cloud top r_E are large, and approach or exceed the detection limit (35 μm), which restricts our analysis somewhat. For 28 June, the differences in the cloud top effective radii between the cumulonimbus in ash free areas (Figure 11, area 1), and the cumulonimbus above Pinatubo (area 2) are very small, with only a slightly lower mean fifth percentile for the ash affected cloud. This is a much smaller effect than for the cases shown by Rosenfeld and Tupper (manuscript in preparation, 2005) for convection growing in ash affected areas, and suggests limited entrainment of the ash particles into the decaying squall line as it reached the Pinatubo area.

[47] However, analysis of the 21 June case shows that the volcanic ash can have a measurable effect on the microphysical structure of the clouds. The monsoonal cloud tops around the entire Pinatubo area (area 4) have a smaller r_E (Figure 12) than the surrounding areas. In this enhancement, the orange-yellow clouds in and south of area 4 are cold cloud tops with r_E of 20–25 μm , and the surrounding red areas are also cold cloud tops, but have r_E of 30 μm or greater. Other analyzed areas in the same image (Figure 11, areas 3 and 5, T/r_E graphs not shown) showed no effect from ash. The effect extends at least 100 km downstream from Pinatubo (to the southwest, in northeasterly upper winds), suggesting a slow aggregation and precipitation rate of the smaller particles. On the coast west of Pinatubo,

a cumulonimbus cell has penetrated the monsoonal cloud tops into the lower stratosphere, to an altitude of about 17 km. From its position and the direction of the “steering” winds, the cloud is of nonvolcanic origin, although possibly partially triggered by downdrafts from the convection over the volcano. Gravity waves radiating from the cell along the tropopause are clearly visible in the image, and may have enhanced transport of the volcanic ash into the stratosphere [Wang, 2003]. The core of the cell has slightly higher r_E than the surrounding cloud, due to enhanced lifting of larger particles in the stronger updrafts, the relative age of the convection, and/or a reduced uptake of ash because of its position in relation to Mount Pinatubo.

[48] A more subtle effect is seen on 15 July (Figure 11c). Because the convection above Pinatubo is completely surrounded by nonvolcanic convection, we can only directly observe the coldest cloud tops. The effect of the aerosols is indicated by a slight, but relatively uniform, change in the enhancement shading over the volcano, and a small drop in r_E near -75°C (Figure 12). No secondary explosions were reported on this day, although Torres *et al.* [1996] report observations taken of an event 2 days earlier. The satellite and available ancillary observations are therefore consistent with the Cubi Point observer’s radar-based interpretation; that ash from the venting mixed with, and was lofted by, cumulonimbi that were convectively enhanced by the Pinatubo environment.

[49] The secondary explosion-produced cloud on 4 September, however, shows no effect on r_E (Figure 11d). Areas 7, 8, and 9 all have $r_E > 35 \mu\text{m}$. Sedimentation effects ensured that the ash deposited closer to the vent from the primary eruptions tended to be coarser than further away [Paladio-Melosantos *et al.*, 1996]. The material injected into the secondary explosion clouds, while containing a sizable proportion of very fine particles from the volcanol-

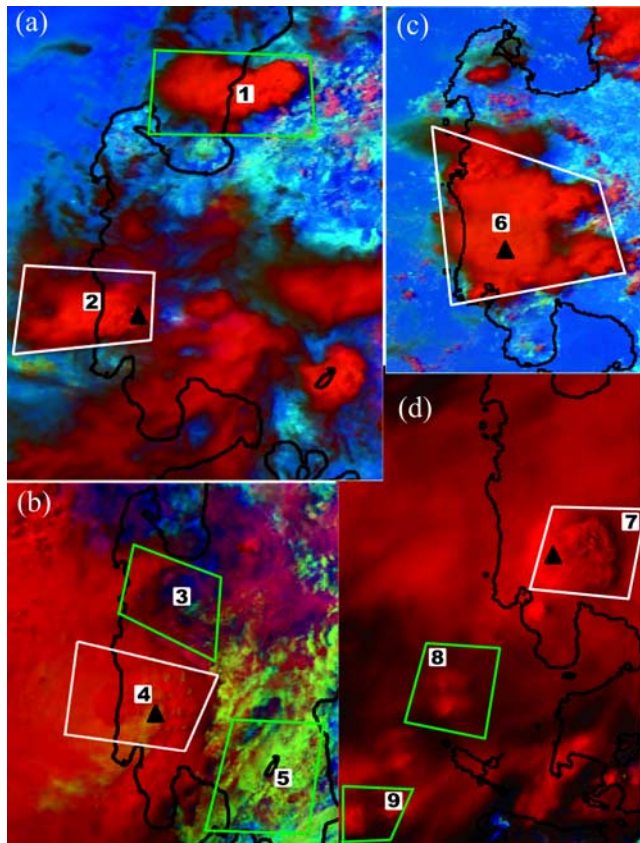


Figure 11. False color NOAA 11 AVHRR imagery for (a) 28 June 1991, 0618 UT (1418 Local Time), (b) 21 June 1991, 0557 UT, (c) 15 July 1991, 0623 UT, (d) 4 September 1991, 0639 UT. The color scheme is described by *Rosenfeld and Lensky* [1998] and used by *Rosenfeld and Tupper* (manuscript in preparation, 2005). The visible reflectance modulates the red, 3.7 μm reflectance modulates the green (more green means more reflectance and smaller cloud particles), and the thermal brightness temperature modulates the blue, where warmer is bluer. Features 1–9 are described in the text; features with a white outline are located over the Pinatubo area, with the location of Pinatubo marked with a black triangle.

ogists' point of view (finer than 4Φ units, or less than $63 \mu\text{m}$) [*Pierson et al.*, 1996; *Torres et al.*, 1996], are still rather large for condensation nuclei. Detailed size data for the finer gradings of secondary explosion ash are not available; however, the distribution had noticeable modes around 7–8 μm and 25–30 μm but drops sharply beyond 6 μm (R. Torres, personal communication, 2004). Thus it is possible that the dominance of giant condensation nuclei in the ash injected from secondary explosions has resulted in quick fallout of the ash and no noticeable effect on r_E . Ash deposition away from the sources of the secondary explosions was relatively small (R. Torres, personal communication, 2004).

[50] From these four cases, all with observed ash emissions into the cloud, it appears that, in addition to the dependence on aerosol flux noted by *Rosenfeld and Tupper* (manuscript in preparation, 2005), the reduction in r_E for

volcanically contaminated clouds is also dependent on the cloud structures and the size of the ash particles.

4. Discussion

4.1. Implications for Volcanic Cloud Monitoring

[51] Many of the world's 1300+ volcanoes are in the moist tropics, in Africa, Southeast Asia, Central and South America [*Simkin*, 1994]. Volcanic clouds from most of these volcanoes are poorly observed, if at all [*Tupper and Kinoshita*, 2003]. Although the Pinatubo eruption was an extreme event and created an unusually large area of pyroclastic deposits, conditions favorable for volcanic-Cbs are possible over a wide area. Even in the midlatitudes, convection over volcanic passive degassing is commonly observed [*Tupper and Kinoshita*, 2003]. In addition to the climatic effect of large eruption clouds which directly inject aerosols to upper tropospheric and stratospheric levels and affect cloud properties [*Minnis et al.*, 1993], we can postulate a possibly significant flux of volcanic ash and/or gases to the upper troposphere and lower stratosphere through moist convection, and an effect on cloud top near-infrared reflectivity which appears to be dependent on mass flux, the convective structure of the clouds, and aerosol sizes.

[52] The height of an eruption has sometimes been used as a proxy for the intensity of an eruption [*Sparks et al.*,

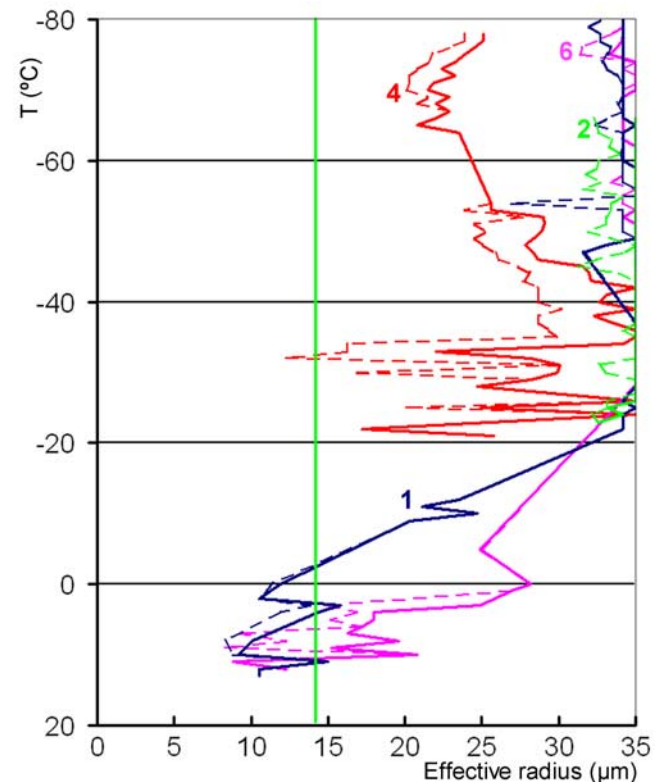


Figure 12. Effective radii for selected numbered areas in Figure 11. Profile 1 is for an area away from Pinatubo; the others are for the Pinatubo region. The fifth (dotted line) and 50th percentiles (solid line) are shown. The vertical line at 14 μm represents the precipitation threshold [*Rosenfeld and Gutman*, 1994].

1997]. For example, to estimate the mass erupted from the climactic Pinatubo eruptions and for the postclimactic radar observations shown here, *Holasek et al.* [1996] used an early conceptual model and the associated altitude and mass flux arguments [*Wilson et al.*, 1978], which neglects the effects of latent heat release in the convective cloud. This method may be appropriate for the climactic eruptions where the heat flux from the eruption is the dominant influence on cloud height, but is possibly inapplicable to the smaller postclimactic events, which may have included volcanic-Cb with mixed origins. Eruption heights in the moist tropics, and particularly where the heights are within the range of ordinary cumulonimbi, should be treated with great caution when used for eruption size estimation. This also applies to the use of these heights in determining the Volcanic Explosivity Index (VEI) [*Newhall and Self*, 1982].

[53] The prevailing attitude of the aviation industry toward volcanic ash is conservative [*Cantor*, 1998]. Aviation operators avoid flying over volcanoes in eruption, and also avoid deep cumulonimbi because of the associated turbulence. However, fine ash detrained from a volcanic-Cb could persist long after the cloud has dissipated. Further examination of these phenomena might result in a revision of International Airways Volcano Watch procedures [*International Civil Aviation Organization*, 2003]. One possible approach is that, where these clouds are explicitly detected, as for the 21 June case here or the cases described by Rosenfeld and Tupper (manuscript in preparation, 2005), explicit SIGMET-type aviation warnings are issued [*Hufford et al.*, 2000]; otherwise the possibility of ash within deep convective cloud could be covered by a longer-term Notice to Airmen (NOTAM).

4.2. Potential for Future Studies

[54] The above observations identify a range of ways that an erupting volcano in a convectively unstable environment can interact with the atmosphere, and particularly the troposphere. Our results are limited by the nature of the observations. Clearly, it would be desirable to quantify some of the areas of uncertainty, to the point where we can more clearly identify the dominant mechanism for convective initiation in each event, the flux of volcanic material into the atmosphere, the composition of the material, and the subsequent effect on microphysical cloud processes.

[55] An intensive meteorological observation period during and following a future major eruption in the moist tropics, in combination with appropriate seismic and infrasound networks, would do much to resolve these uncertainties. *Oswalt et al.* [1996] suggested the use of van-based mobile Doppler weather radar, with appropriate calibration and range and azimuth recording. Cheap and relatively expendable, ground-based camera systems could be deployed immediately after activity was noted [*Kinoshita et al.*, 2004], pending the construction of secure facilities for more expensive sensors. Direct aircraft sampling would reveal much about the cloud properties and has been successfully performed before in volcanic clouds despite the associated risk of damage [*Obenholzer et al.*, 2003; *Zinster*, 1994]. Robotic aircraft [*Holland et al.*, 2001] with an appropriate meteorological payload could also be used. New generation satellite sensors (e.g., MODIS or Meteosat

second generation) will extend the range and frequency of cloud measurements possible, and Lidars could be used to identify layers of aerosols lofted in the clouds.

[56] To perform such detailed observations during and after a volcanic crisis would require close cooperation between the volcanological and meteorological research and operational communities, and the government of the country most affected. *Rodolfo* [1995] gives an account of some perceived mistakes during parts of the Pinatubo crisis, which was in many other respects a model for international cooperation. Guidelines for behavior of visiting scientists during a volcanic crisis have already been drafted and should be followed by all parties involved in a future study [*International Association of Volcanology and Chemistry of the Earth's Interior*, 1999].

[57] Atmospheric models have already been used to simulate mesoscale environmental processes around a volcano [*Favalli et al.*, 2004]. To examine the role of volcanic particles within the deep convection, it will be possible to use a nonhydrostatic, nonsteady state, high-resolution atmospheric model such as ATHAM [*Graf et al.*, 1999], which has also been used to simulate low-level biomass burning plumes [*Trentmann et al.*, 2002], and microphysical processes within an eruption column [*Textor et al.*, 2003]. Development of these models will require close ground truthing from the further observations discussed above.

5. Conclusions

[58] Satellite observations clearly identify the area of enhanced convection described by *Oswalt et al.* [1996] in the months following the 15 June 1991 Pinatubo eruption. The dominant effect of the heat and emissions from the volcano was to increase convection in all hours and to make the diurnal peak in convection over the Pinatubo area in June–September 1991 2–3 hours earlier in the afternoon than over surrounding areas, or over the same area 11 years later. A range of possible mechanisms has been identified. In addition to the localized processes for triggering convection, such as secondary phreatic explosions, eruption clouds in the lower troposphere, and the heat from bare volcanic deposits, the broader synoptic-scale meteorological environment plays an important role, by influencing the broad-scale instability of the atmosphere and the generation of orographic convection.

[59] In one event, on 21 June 1991, the clouds contaminated by venting from the volcano had a significant reduction in cloud top particle effective radii. Less significant effects were noted for two other cases. The cloud triggered from a large secondary phreatic explosion on 4 September 1991 appeared to have relatively normal cloud top effective radii, perhaps because of the dominance of large particle sizes injected into the cloud.

[60] These results demonstrate that volcanic eruptions into the atmosphere can, through triggering moist convection, inject volcanic emissions to any height within the troposphere or lower stratosphere, given the appropriate meteorological environment. Further observational and theoretical work may improve the sensitivity and timeliness of remote sensing of these events, clarify the flux of volcanic ash or gases into the upper troposphere and lower strato-

sphere following major or during more minor eruptions, and help mitigate the risk to aviation.

[61] **Acknowledgments.** Much of this research was conducted while A. Tupper was a guest at Kagoshima University, Kyushu, Japan. The study was partially supported by the Israeli Space Agency. Omer Burshtein of the Hebrew University assisted with the microphysical analyses. David Howard of the Bureau of Meteorology extracted the GMS data. We are grateful to three anonymous reviewers and to Kisei Kinoshita, Chikara Kanagaki, Naoko Iino, Megumi Koyamada, Chris Newhall, Rodney Potts, Jim Arthur, Geoffrey Garden, Christiane Textor, Gerald Ernst, Ronnie Torres, Earle Williams, and Michael Reeder for their comments and support.

References

- Adug, E. A. (2001), Tropical Weather Systems affecting the Philippines, in *International Workshop on the Dynamics and Forecasting of Tropical Weather Systems*, edited by G. Jackson, pp. 44–51, Bur. of Meteorol., Darwin, Australia.
- Cantor, R. (1998), Complete avoidance of volcanic ash is only procedure that guarantees flight safety, *ICAO Mag.*, 53, 18–19, 26.
- Carello, P. T., B.-K. Cheang, and H.-V. Tan (1994), The tropical circulation in the Australian/Asian region: May to October 1991, *Aust. Meteorol. Mag.*, 43, 193–203.
- Casadevall, T. J. (1994), The 1989–1990 eruption of Redoubt Volcano, Alaska: Impacts on aircraft operations, *J. Volcanol. Geotherm. Res.*, 62, 301–316.
- Casadevall, T. J., P. J. Delos Reyes, and D. J. Schneider (1996), The 1991 Pinatubo eruptions and their effects on aircraft operations, in *Fire and Mud: Eruptions and Lahars of Mount Pinatubo, Philippines*, edited by C. G. Newhall and R. S. Punongbayan, pp. 625–636, Univ. of Wash. Press, Seattle.
- Dalida, L. U., and I. I. Valeroso (1999), Thunderstorm hazard mapping in the Philippines, 34 pp., Nat. Disaster Reduction Branch, Philippine Atmos., Geophys. and Astron. Serv. Admin., Quezon City.
- Ellrod, G. P., B. H. Connell, and D. W. Hillger (2003), Improved detection of airborne volcanic ash using multispectral infrared satellite data, *J. Geophys. Res.*, 108(D12), 4356, doi:10.1029/2002JD002802.
- Emanuel, K. A. (1994), *Atmospheric Convection*, 592 pp., Oxford Univ. Press, New York.
- Favalli, M., F. Mazzarini, M. Pareschi, and E. Boshci (2004), Role of the local wind circulation in plume monitoring at Mt. Etna volcano (Sicily): Insights from a mesoscale numerical model, *Geophys. Res. Lett.*, 31, L09105, doi:10.1029/2003GL019281.
- Fromm, M. D., and R. Servranckx (2003), Transport of forest fire smoke above the tropopause by supercell convection, *Geophys. Res. Lett.*, 30(10), 1542, doi:10.1029/2002GL016820.
- Fromm, M., A. Tupper, L. Poole, R. Servranckx, R. Bevilacqua, and D. Rosenfeld (2003), Stratospheric smoke down under: Injection from Australian fires/convection in January 2003, *Eos Trans. AGU*, 84(46), Fall Meet. Suppl., Abstract A11C-05.
- Graf, H., M. Herzog, J. M. Oberhuber, and C. Textor (1999), Effect of environmental conditions on volcanic plume rise, *J. Geophys. Res.*, 104, 24,309–24,320.
- Grindle, T. J., and F. W. Burcham (2003), Engine damage to a NASA DC-8-72 airplane from a high-altitude encounter with a diffuse volcanic ash cloud, 22 pp., NASA, Edwards, Calif.
- Guo, S., W. I. Rose, G. J. S. Bluth, and I. M. Watson (2004a), Particles in the great Pinatubo volcanic cloud of June 1991: The role of ice, *Geochem. Geophys. Geosyst.*, 5, Q05003, doi:10.1029/2003GC000655.
- Guo, S., G. J. S. Bluth, W. I. Rose, I. M. Watson, and A. J. Prata (2004b), Reevaluation of SO₂ release of the 15 June 1991 Pinatubo eruption using ultraviolet and infrared satellite sensors, *Geochem. Geophys. Geosyst.*, 5, Q04001, doi:10.1029/2003GC000654.
- Hoblitt, R. P., E. W. Wolfe, W. E. Scott, M. R. Couchman, J. S. Pallister, and D. Javier (1996), The preclimatic eruptions of Mount Pinatubo, June 1991, in *Fire and Mud: Eruptions and Lahars of Mount Pinatubo, Philippines*, edited by C. G. Newhall and R. S. Punongbayan, pp. 457–511, Univ. of Wash. Press, Seattle.
- Holasek, R. E., S. Self, and A. W. Woods (1996), Satellite observations and interpretation of the 1991 Mount Pinatubo eruption plumes, *J. Geophys. Res.*, 101, 27,635–27,665.
- Holland, G. J., et al. (2001), The Aerosonde robotic aircraft: A new paradigm for environmental observations, *Bull. Am. Meteorol. Soc.*, 82, 889–901.
- Houze, R. A. (1994), *Cloud Dynamics*, 573 pp., Elsevier, New York.
- Hufford, G. L., L. J. Salinas, J. J. Simpson, E. G. Barske, and D. C. Pieri (2000), Operational implications of airborne volcanic ash, *Bull. Am. Meteorol. Soc.*, 81, 745–755.
- International Association of Volcanology and Chemistry of the Earth's Interior (IAVCEI) (1999), Report by IAVCEI Subcommittee for Crisis Protocols, Professional conduct of scientists during volcanic crises, *Bull. Volcanol.*, 60, 323–334.
- International Civil Aviation Organization (2000), *Handbook on the International Airways Volcano Watch (IAVW)*, 120 pp., Montreal.
- International Civil Aviation Organization (2003), *Handbook on the International Airways Volcano Watch (IAVW)*, 2nd ed., 34 pp., Montreal.
- Johnson, R. W., and T. J. Casadevall (1994), Aviation safety and volcanic ash clouds in the Indonesia-Australia region, in *First International Symposium on Volcanic Ash and Aviation Safety*, edited by T. J. Casadevall, *U.S. Geol. Surv. Bull.*, 2047, 191–197.
- Joint Typhoon Warning Center (1991), *1991 Annual Tropical Cyclone Report*, 238 pp., U.S. Nav. Oceanogr. Command Cent., Guam, Mariana Islands.
- Joint Typhoon Warning Center (2002), *2002 Annual Tropical Cyclone Report*, Nav. Pac. Meteorol. and Oceanogr. Cent./Joint Typhoon Warning Cent., Pearl Harbor, Hawaii.
- Kinoshita, K., C. Kanagaki, N. Iino, M. Koyamada, A. Terada, and A. Tupper (2002), Volcanic plumes at Miyakejima observed from satellites and from the ground, in *Optical Remote Sensing of the Atmosphere and Clouds III*, edited by H.-L. Huang, D. Lu, and Y. Sasano, pp. 227–236, Int. Soc. for Opt. Eng., Bellingham, Wash.
- Kinoshita, K., et al. (2004), Ground and satellite monitoring of volcanic aerosols in visible and infrared bands, paper presented at the CERES International Symposium on Remote Sensing: Monitoring of Environmental Change in Asia, 16–17 Dec., Chiba, Japan.
- Lynch, J. S., and G. Stephens (1996), Mount Pinatubo: A Satellite Perspective of the June 1991 Eruptions, in *Fire and Mud: Eruptions and Lahars of Mount Pinatubo, Philippines*, edited by C. G. Newhall and R. S. Punongbayan, pp. 637–645, Univ. of Wash. Press, Seattle.
- Meteorological Satellite Center (1989), *GMS Users' Guide*, 2nd ed., Jpn. Meteorol. Agency, Tokyo.
- Minnis, P., E. F. Harrison, L. L. Stowe, G. G. Gibson, F. M. Denn, D. R. Doelling, and W. Smith (1993), Radiative climate forcing by the Mount Pinatubo eruption, *Science*, 259, 1411–1415.
- Mori, J., et al. (1996), Volcanic earthquakes following the 1991 climatic eruption of Mount Pinatubo: Strong seismicity during a waning eruption, in *Fire and Mud: Eruptions and Lahars of Mount Pinatubo, Philippines*, edited by C. G. Newhall and R. S. Punongbayan, pp. 339–350, Univ. of Wash. Press, Seattle.
- National Oceanic and Atmospheric Administration (1998), *Polar orbiter data user's guide*, Silver Spring, Md.
- Newhall, C. G., and S. Self (1982), The volcanic explosivity index (VEI): An estimate of explosive magnitude for historical volcanism, *J. Geophys. Res.*, 87, 1231–1238.
- Obenholzer, J. H., H. Schroettner, P. Golob, and H. Delgado (2003), Particles from the plume Popocatepetl volcano, Mexico: The FESEM/EDS approach, in *Volcanic Degassing*, edited by C. Oppenheimer, D. M. Pyle, and J. Barclay, *Geol. Soc. Spec. Publ.*, 213, 123–148.
- Okumura, K., T. Satomura, T. Oki, and W. Khantiyanan (2003), Diurnal variation of precipitation by moving mesoscale systems: Radar observations in northern Thailand, *Geophys. Res. Lett.*, 30(20), 2073, doi:10.1029/2003GL018302.
- Oswalt, J. S., W. Nichols, and J. F. O'Hara (1996), Meteorological observations of the 1991 Mount Pinatubo eruption, in *Fire and Mud: Eruptions and Lahars of Mount Pinatubo, Philippines*, edited by C. G. Newhall and R. S. Punongbayan, pp. 625–636, Univ. of Wash. Press, Seattle.
- Paladio-Melosantos, M. L. O., et al. (1996), Tephra falls of the 1991 eruptions of Mount Pinatubo, in *Fire and Mud: Eruptions and Lahars of Mount Pinatubo, Philippines*, edited by C. G. Newhall and R. S. Punongbayan, pp. 513–535, Univ. of Wash. Press, Seattle.
- Pierson, T. C., A. S. Daag, P. J. D. Reyes, M. T. M. Regalado, R. U. Solidum, and B. S. Tubianosa (1996), Flow and deposition of post-eruption hot lahars on the east side of Mount Pinatubo, July–October 1991, in *Eruptions and Lahars of Mount Pinatubo, Philippines*, edited by C. G. Newhall and R. S. Punongbayan, pp. 921–950, Univ. of Wash. Press, Seattle.
- Pinatubo Volcano Observatory Team (1991), Lessons from a major eruption: Mt. Pinatubo, Philippines, *Eos*, 72, 545, 552–555.
- Potts, R. J. (1993), Satellite observations of Mt Pinatubo ash clouds, *Aust. Meteorol. Mag.*, 42, 59–68.
- Prata, A. J. (1989a), Infrared radiative transfer calculations for volcanic ash clouds, *Geophys. Res. Lett.*, 16, 1293–1296.
- Prata, A. J. (1989b), Observations of volcanic ash clouds in the 10–12 μ m window using AVHRR/2 data, *Int. J. Remote Sens.*, 10, 751–761.
- Prata, A. J., G. J. S. Bluth, W. I. Rose, D. J. Schneider, and A. C. Tupper (2001), Comments on “Failures in detecting volcanic ash from a satellite-based technique”, *Remote Sens. Environ.*, 78, 341–346.

- Robock, A. (2002), Pinatubo eruption: The climatic aftermath, *Science*, 295, 1242–1244.
- Rodolfo, K. S. (1995), *Pinatubo and the Politics of Lahar: Eruption and Aftermath, 1991*, 341 pp., Univ. of the Philippines, Quezon City.
- Rose, W. I., et al. (1995), Ice in the 1994 Rabaul eruption cloud: Implications for volcano hazard and atmospheric effects, *Nature*, 375, 477–479.
- Rosenfeld, D., and G. Gutman (1994), Retrieving microphysical properties near the tops of potential rain clouds by multispectral analysis of AVHRR data, *J. Atmos. Res.*, 34, 259–283.
- Rosenfeld, D., and I. M. Lensky (1998), Spaceborne sensed insights into precipitation formation processes in continental and maritime clouds, *Bull. Am. Meteorol. Soc.*, 79, 2457–2476.
- Rudich, Y., A. Sagi, and D. Rosenfeld (2003), Influence of the Kuwait oil fires plume (1991) on the microphysical development of clouds, *J. Geophys. Res.*, 108(D15), 4478, doi:10.1029/2003JD003472.
- Sawada, Y. (1987), *Study on Analysis of Volcanic Eruptions Based on Eruption Cloud Image Data Obtained by the Geostationary Meteorological Satellite (GMS)*, 335 pp., Meteorol. Res. Inst., Tokyo.
- Sawada, Y. (2003), Study on observation and analysis of eruption cloud with imagery of Geostationary Meteorological Satellite, Himawari, *J. Meteorol. Res.*, 55, 57–152.
- Seidel, D. J., R. J. Ross, J. K. Angell, and G. C. Reid (2001), Climatological characteristics of the tropical tropopause as revealed by radiosondes, *J. Geophys. Res.*, 106, 7857–7878.
- Shaik, H. A., and G. E. Jackson (2003), The tropical circulation in the Australian/Asian region: May to October 2002, *Aust. Meteorol. Mag.*, 52, 189–201.
- Simkin, T. (1994), Volcanoes: Their occurrence and geography, in *First International Symposium on Volcanic Ash and Aviation Safety*, edited by T. J. Casadevall, *U.S. Geol. Surv. Bull.*, 2047, 75–79.
- Sparks, R. S. J., M. I. Bursik, S. N. Carey, J. E. Gilbert, L. Glaze, H. Sigurdsson, and A. W. Woods (1997), *Volcanic Plumes*, 589 pp., John Wiley, Hoboken, N. J.
- Textor, C., H.-F. Graf, M. Herzog, and J. M. Oberhuber (2003), Injection of gases into the stratosphere by explosive volcanic eruptions, *J. Geophys. Res.*, 108(D19), 4606, doi:10.1029/2002JD002987.
- Tokuno, M. (1991), GMS-4 Observations of volcanic eruption clouds from Mt. Pinatubo, Philippines, 14 pp., Jpn. Meteorol. Agency Meteorol. Sat. Cent., Tokyo.
- Torres, R. C., S. Self, and M. M. L. Martinez (1996), Secondary pyroclastic flows from the June 15, 1991, ignimbrite of Mount Pinatubo, in *Fire and Mud: Eruptions and Lahars of Mount Pinatubo, Philippines*, edited by C. G. Newhall and R. S. Punongbayan, pp. 665–678, Univ. of Wash. Press, Seattle.
- Trentmann, J., M. O. Andreae, H.-F. Graf, P. V. Hobbs, R. D. Ottmar, and T. Trautmann (2002), Simulation of a biomass-burning plume: Comparison of model results with observations, *J. Geophys. Res.*, 107(D2), 4013, doi:10.1029/2001JD000410.
- Tupper, A., and K. Kinoshita (2003), Satellite, air and ground observations of volcanic clouds over islands of the southwest Pacific, *South Pac. Study*, 23, 21–46.
- Tupper, A., S. Carn, J. Davey, Y. Kamada, R. Potts, F. Prata, and M. Tokuno (2004), An evaluation of volcanic cloud detection techniques during recent significant eruptions in the western ‘Ring of Fire’, *Remote Sens. Environ.*, 91, 27–46, doi:10.1016/j.rse.2004.02.004.
- Wang, P. K. (2003), Moisture plumes above thunderstorm anvils and their contributions to cross-tropopause transport of water vapor in midlatitudes, *J. Geophys. Res.*, 108(D6), 4194, doi:10.1029/2002JD002581.
- Wilson, L. S., R. S. J. Sparks, T. C. Huang, and N. D. Watkins (1978), The control of volcanic column heights by eruption energetics and dynamics, *J. Geophys. Res.*, 83, 1829–1836.
- Wolfe, E. W., and R. P. Hoblitt (1996), Overview of the Eruptions, in *Fire and Mud: Eruptions and Lahars of Mount Pinatubo, Philippines*, edited by C. G. Newhall and R. S. Punongbayan, pp. 3–20, Univ. of Wash. Press, Seattle.
- Woods, A. W. (1993), Moist convection and the injection of volcanic ash into the atmosphere, *J. Geophys. Res.*, 98, 17,627–17,636.
- Woods, A. W. (1998), Observations and models of volcanic eruption columns, in *The Physics of Explosive Volcanic Eruptions*, edited by J. S. Gilbert and R. S. J. Sparks, *Geol. Soc. Spec. Publ.*, 145, 91–114.
- Wu, R., and B. Wang (2001), Multi-stage onset of the summer monsoon over the western North Pacific, *Clim. Dyn.*, 17, 277–289.
- Yasunaga, K., H. Kida, T. Satomura, and N. Nishi (2004), A numerical study on the detrainment of tracers by cumulus convection in TOGA COARE, *J. Meteorol. Soc. Jpn.*, 82, 861–878.
- Zinster, L. M. (1994), Effects of volcanic ash on aircraft powerplants and airframes, in *First International Symposium on Volcanic Ash and Aviation Safety*, edited by T. J. Casadevall, *U.S. Geol. Surv. Bull.*, 2047, 141–145.

J. S. Oswalt, 308 Suffolk Drive, Long Beach, MS 39650-2601, USA. (jamesoswalt@cableone.net)

D. Rosenfeld, Institute of Earth Sciences, Department of Atmospheric Sciences, Hebrew University of Jerusalem, Givat Ram, Jerusalem, 91904 Israel. (daniel@vms.huji.ac.il)

A. Tupper, Bureau of Meteorology, Darwin, Australia, and Monash University, P.O. Box 40050, Casuarina, Northern Territory 0811, Australia. (a.tupper@bom.gov.au)